DOI 10.1007/s11237-015-9422-x
Theoretical and Experimental Chemistry, Vol. 51, No. 4, September, 2015 (Russian Original Vol. 51, No. 4, July-August, 2015)

EFFECT OF THE CARBON SUPPORT ON THE CATALYTIC ACTIVITY OF PLATINUM NANOPARTICLES IN THE WATER GAS SHIFT REACTION

Z. V. Kaidanovych,[1] Ye. Yu. Kalishyn,[1] V. I. Grytsenko,[1] G. R. Kosmambetova,[1] D. A. Zyuzin,[2] E. M. Moroz,[2] and P. E. Strizhak[1]

UDC 544.478.1

Platinum nanoparticles supported on carbon nanotubes display higher activity in the water gas shift reaction with close to 100% conversion of CO at 400-450 °C than for platinum supported on SKT activated carbon. A TEM study showed that this effect may be attributed to stabilization of the platinum nanoparticles on the surface of the carbon nanotubes, which prevents their agglomeration during the reaction.

Key words: *platinum nanoparticles, water gas shift reaction, carbon nanotubes.*

The water gas shift reaction ($CO + H_2O \leftrightarrow CO_2 + H_2 + \Delta H$, $\Delta H = 41.2$ kJ/mol) is an important stage in the generation of hydrogen from organic matter, leading to hydrogen enrichment of the reforming mixture and a reduction in the amount of CO [1]. In several cases as in the industrial production of hydrogen from methane, the removal of CO from hydrogen through the water gas shift reaction involves two steps: 1) a high-temperature step using iron-containing catalysts and 2) a low-temperature step using copper-containing systems. On the whole, the CO content can be reduced down to 1%-2% [2]. Interest in systems based on expensive noble metals has arisen due to the need to find efficient and heat-stable catalysts for compact fuel devices, in which this process may be carried out in a single step [3, 4]. The nature of the support and size of the active component particles are factors determining the activity of these catalysts [4, 5]. Oxides of aluminum, cerium, zirconium, and titanium are mainly used as supports [6]. There is hardly any information in the literature on the use of carbon nanotubes (CNT) for this process. Menon et al. [7] have reported improved magnetic, mechanical, and electroconducting properties of such composite materials relative to analogous systems based on amorphous carbon due to the interaction of the transition metals with carbon nanotubes. The introduction of 44% CNT into a cerium-lanthanum oxide support of a platinum catalyst enhances its activity in the water gas shift reaction due to formation of more dispersed platinum crystallites on segments of the CNT, an increase in the concentration of carbon-containing intermediates in the activated complex, a reduction in the Pt—CO bond energy, an increase in the reducibility of the cerium–lanthanum support, and an increase in the platinum dispersion along with decreased size of the support crystallites in the presence of CNT [8].

[1]L. V. Pisarzhevskii Institute of Physical Chemistry, National Academy of Sciences of Ukraine, Prospekt Nauky, 31, Kyiv 03028, Ukraine. E-mail: z.kaidanovych@gmail.com.
[2]Boreskov Institute of Catalysis, Siberian Branch, Russian Academy of Sciences, Prospekt Akademika Lavrentieva, 5, Novosibirsk 630090, Russian Federation.

Translated from Teoreticheskaya i Éksperimental'naya Khimiya, Vol. 51, No. 4, pp. 230-235, July-August, 2015. Original article submitted July 9, 2015.

In the present work, we studied the catalytic properties of composite systems derived from platinum nanoparticles and carbon materials in the water gas shift reaction as potential catalysts for compact fuel processes. Carbon nanotubes (CNT) obtained by catalytic pyrolysis and SKT activated carbon were used as the supports.

EXPERIMENTAL

SKT activated carbon and carbon nanotubes prepared by the catalytic pyrolysis of ethylene on Ni/CaO and Co/CaO catalysts were used in preparation of the catalysts [9]. The resultant nanotubes were purified by heating in excess concentrated nitric acid at reflux, subsequent washing with distilled water, and drying at 200 °C.

Colloidal solutions of platinum nanoparticles stabilized by polyvinylpyrrolidone were prepared according to a reported procedure [10, 11].

The platinum nanoparticles were deposited by mixing a corresponding amount of a colloidal solution of platinum nanoparticles in ethanol and the support followed by subsequent evaporation at 75 °C with periodic stirring and drying at 120 °C for 4 h. The content of platinum nanoparticles in the catalysts was determined by X-ray fluorescence analysis (1%). The following designations are used for the catalyst samples: Pt/SKT) platinum nanoparticles supported on SKT activated carbon, Pt/CNT-25) platinum nanoparticles supported on carbon nanotubes obtained on a Co/CaO catalyst, and Pt/CNT-35) platinum nanoparticles supported on carbon nanotubes obtained on an Ni/CaO catalyst.

The morphology of the catalysts and supports was studied by transmission electron microscopy using a PÉM-125K electron microscope.

The phase composition and size of the coherent scattering regions (CSR) were determined by X-ray diffraction using an HZG-4C diffractometer and monochromatized copper radiation with wavelength K_α = 1.5418 Å. Qualitative phase analysis was carried out using the X-ray diffraction data file (Version 1.30, August, 1997, JCPDS-ICDD and Inorganic Crystal Structure Data Base, 2003-2011 Fachinformationszentrum (Fiz) Karlsruhe).

The catalytic properties in the water gas shift reaction were studied in a flow reactor at pressure 0.1 MPa, 200-450 °C, and volumetric flow velocity 12000 h^{-1} and partial pressures for the gas mixture P_{CO} = 4 kPa, P_{H_2O} = 21 kPa, P_{He} = 75 kPa. The sample mass was 0.15 g. Analysis for CO and CO_2 was carried out on an LKhM-80MD gas chromatograph.

The rate of the water gas shift reaction was calculated using the formula

$$r = \frac{C_{CO_2} V_{tot}}{22.4 m_{Pt}}$$

where C_{CO_2} is the mole fraction of CO_2, V_{tot} is the total gas mixture flow, L/s, m_{Pt} is the mass of platinum in the sample, g, and 22.4 is the molar volume, L/mol.

RESULTS AND DISCUSSION

TEM images of platinum nanoparticles supported on SKT and carbon nanotubes are given in Fig. 1a,c. The mean diameter of the platinum nanoparticles was 5.5 nm. In all cases, the size distribution of the platinum nanoparticles was monodisperse. We should note that carbon nanotube surface features mainly isolated platinum nanoparticles, which are very clearly evident in the TEM images. Both isolated platinum nanoparticles and nanoparticle agglomerations are present on the SKT surface.

Diffraction patterns of the carbon-containing supports are given in Fig. 2a. A reflection was found for all the supports in the vicinity of 2θ = 25° which corresponds to the [002] crystallographic plane of graphite. The diffraction pattern of CNT-25 shows reflections with 2θ = 45° and 54°, which are related to the metallic cobalt phase. The diffraction pattern for the CNT-35 support contains peaks at 2θ = 45° and 52°, which correspond to metallic nickel. The nickel and cobalt phases found in the carbon nanotubes are residues of the catalysts used in the preparation of these supports. The ash content of the nanotubes used

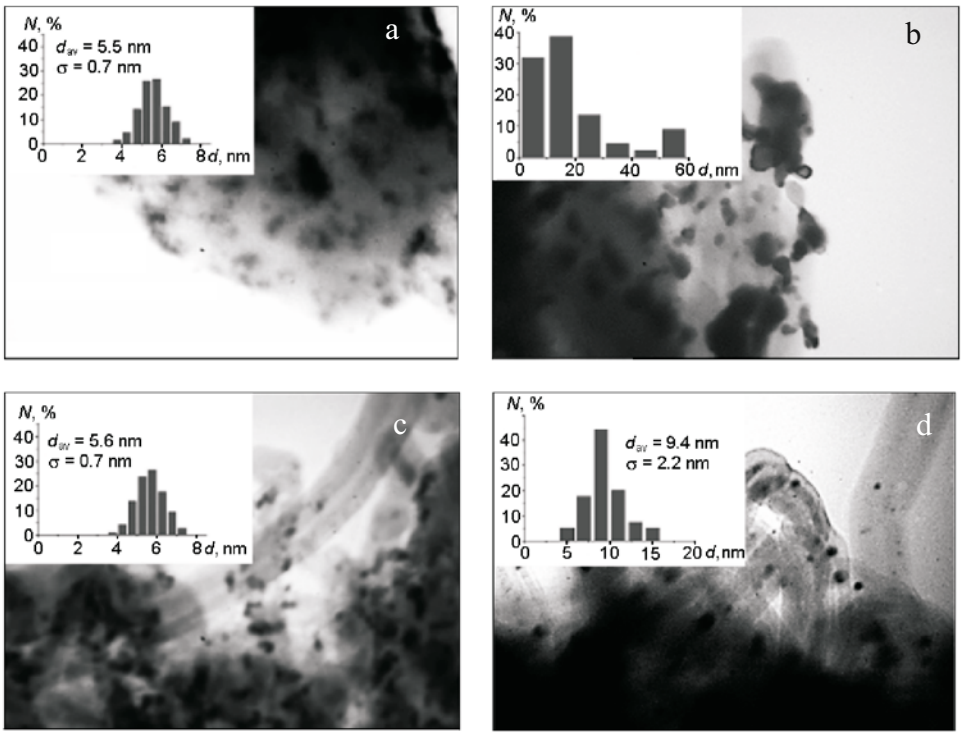

Fig. 1. TEM images of platinum nanoparticles: a, b) supported on SKT before and after the reaction, respectively, c, d) supported on carbon nanotubes before and after the reaction, respectively. The inserts give the size distribution of the platinum nanoparticles. *N*) number of particles, d_{av}) average nanoparticle diameter, σ) mean-square deviation.

was up to 3%. Tsang et al. [12] had already shown that cobalt and nickel nanoparticles are encapsulated within the nanotubes and have no effect on the catalytic activity of the CNT.

Diffraction patterns of platinum catalysts supported on SKT and carbon nanotubes are shown in Fig. 2b. In addition to the reflections for carbon, nickel, and cobalt, which are present in the diffraction patterns of the supports (Fig. 2a), peaks are found for metallic platinum at $2\theta = 39.78°$ in the patterns for the catalysts. The CSR of the platinum particles for all the catalysts are 5.0-5.5 nm.

Table 1 gives the structural characteristics for the carbon supports. These data indicate that activated carbon has a well-developed specific surface area (970 m^2/g). The diameter of the carbon nanotubes determined from the TEM images was 35 nm for the CNT-35 sample but only 25 nm for the CNT-25 sample. The CNT-35 and CNT-25 samples have specific surface area 85 and 150 m^2/g, respectively. The CSR for the graphite phase D_{002} in the carbon nanotubes are similar: 5.0 nm for CNT-25 and 5.5 nm for CNT-35. The CSR for the activated carbon ($D_{002} < 2.0$ nm) is shorter than for the nanotubes. Such CSR values indicate that the wall thickness of the carbon nanotubes is 5.0-5.5 nm, while graphite phase crystallites exist in the SKT structure with diameter up to 2 nm.

Table 2 gives data for the size of the supported platinum nanoparticles determined by electron microscopy and the size of the CSR of the platinum nanoparticles. The diameters of the platinum nanoparticles determined by TEM and the size of the CSR of the platinum nanoparticles are approximately the same for all the catalysts (5.5 nm). Thus, electron microscopy and X-ray diffraction showed that the size of the platinum nanoparticles in the catalysts corresponds to the dimensions in the colloidal solution and is not a function of the carbon support.

The catalytic properties of the carbon supports and the catalysts made with these supports were studied in the water gas shift reaction at 200-450 °C. SKT is inactive in the water gas shift reaction. Carbon nanotubes display activity above 400 °C, but the conversion of CO under these reaction conditions does not exceed 15%.

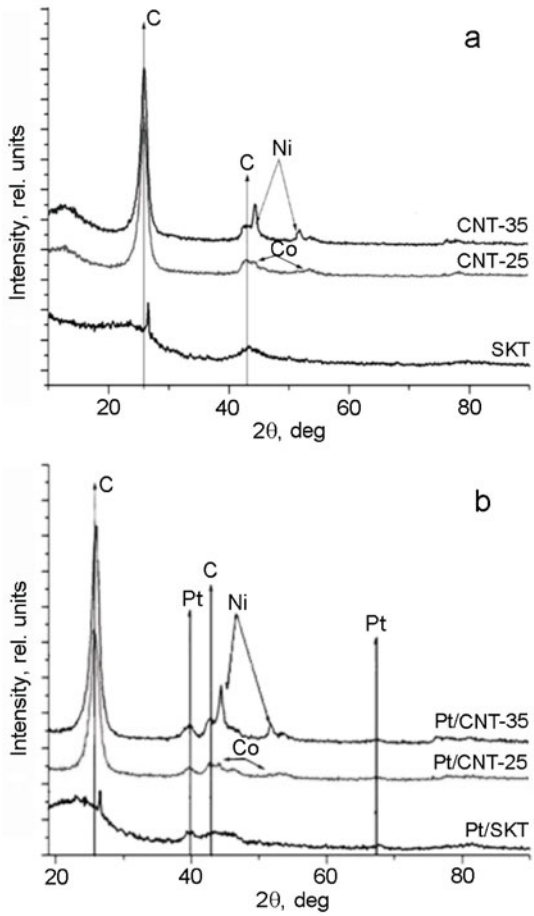

Fig. 2. Diffraction patterns of the supports (a) and catalysts (b).

Curves for the temperature dependence of the CO conversion on the platinum catalysts are given in Fig. 3a. The conversion of CO on the catalyst with platinum nanoparticles supported on SKT at 200-450 °C does not exceed 10%. The slight activity of the Pt/SKT catalyst is in accord with literature data. Buitrago et al. [13] have shown that platinum supported on activated carbon with surface area 1487 m^2/g does not display activity in the water gas shift reaction. In contrast to Pt/SKT, platinum catalysts with carbon nanotubes as the support are active in this reaction. Complete conversion of CO is achieved at 350 °C on Pt/CNT-35 and at 400 °C on Pt/CNT-25. The higher activity for the catalysts made with platinum supported on CNT may be attributed to features of the interaction of platinum and the carbon nanotubes. We should note that our results on Pt/CNT catalysts proved reproducible upon repeating the experiment.

In order to elucidate the differences in the metal–carbon support interaction, the catalyst samples were studied after testing in the water gas shift reaction. TEM images for samples of Pt/SKT and Pt/CNT-35 after catalysis are presented in Fig. 1b, d. Analysis of the TEM image for the Pt/SKT sample (Fig. 1b) shows that the platinum nanoparticles sinter during the reaction that results in formation of agglomerates with diameter from 10 to 60 nm. The mean diameter of the platinum nanoparticles supported on CNT is 9.4 nm and the mean-square deviation is 2.2 nm. The shape of the size distribution is unchanged (Fig. 1d). Thus, comparison of the TEM images of the samples after use in catalysis shows that the thermal stability of the catalysts with platinum supported on CNT is much higher than for the samples with SKT as the support. Lee et al. [14] have reported that the high stability of Pt/CNT electrocatalysts in comparison with Pt/SKT is related to a stronger interaction of platinum and carbon on the CNT surface.

TABLE 1. Specific Surface Area, CSR Diameters of the Supports, and Internal Nanotube Diameter

Sample	Specific surface area, m^2/g	CSR, D_{002}, nm	Average diameter (TEM), nm
CNT-35	85	5.5	35
CNT-25	150	5.0	25
SKT	970	<2.0	

TABLE 2. Mean Diameter of the Platinum Nanoparticles and CSR Dimensions

Sample	Pt CSR, nm	Average Pt diameter (TEM), nm
Pt/SKT	5.0	5.5
Pt/CNT-25	5.5	5.6
Pt/CNT-35	5.0	5.6

In order to compare the catalytic activity of the samples, we calculated the rate of the water gas shift reaction on the hybrid nanomaterials, Pt/CNT and Pt/SKT relative to the mass of supported platinum for low conversions (Fig. 3b). Our data show that the rate of CO conversion at 300 °C on the Pt/CNT catalysts is 10 times greater than the corresponding value for the Pt/SKT catalyst. We should note that the Pt/CNT-25 sample with larger surface area than for Pt/CNT-35 displays greater catalytic activity.

The difference in the catalytic activities of catalysts Pt/SKT and Pt/CNT may be attributed to the greater metal–support interaction stabilizing the platinum nanoparticles on the CNT surface in comparison with Pt/SKT. This discrepancy may be the result of greater electron conduction for the carbon nanotubes in comparison due to the presence of graphene layers. The reaction of platinum and the CNT surface leads to an additional interaction with the π-orbital of the CO molecule and, as a consequence, enhanced catalytic activity [15-17].

We should also note that the activity of Pt/CNT catalysts in the water gas shift reaction, in contrast to Pt/SKT, may also be attributed to the large external surface and very small amount of micropores in the carbon nanotubes. Such CNT properties provide for accessibility to the active sites and are favorable for the diffusion of reagents or products [18, 19]. Thus, Onoe et al. [19] have established that platinum nanoparticles on activated carbon is found in the support micropores, while the nanoparticles on CNT are located on the accessible external surface of the nanotubes. As a result, Pt/CNT catalysts display higher catalytic activity in the hydrogenation of nitrobenzene and also C=C bonds in organic compounds than for platinum supported on activated carbon [18, 19].

Thus, we have studied the physicochemical and catalytic properties of some composite nanomaterials. These catalysts were obtained by the deposition of previously formed platinum nanoparticles with mean diameter 5.6 nm on carbon nanotubes and SKT activated carbon. TEM and XRD were used to show that the mean platinum nanoparticle diameter was virtually unchanged upon deposition onto the support. However, mainly isolated platinum nanoparticles exist on the surface of the

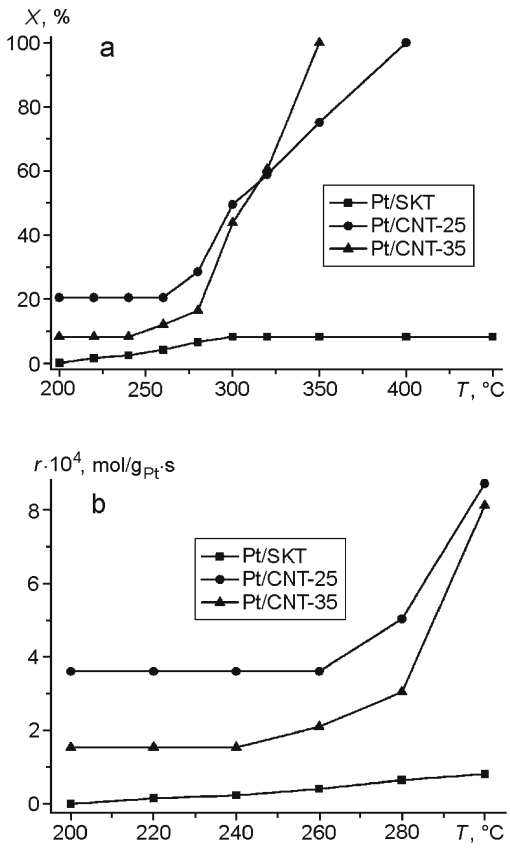

Fig. 3. Temperature dependence of the CO conversion (a) and water gas shift reaction rate (b). Experimental conditions: pressure 0.1 MPa, volumetric flow velocity 12,000 h^{-1}, $P_{CO} = 4$ kPa, $P_{H_2O} = 21$ kPa, and $P_{He} = 75$ kPa.

carbon nanotubes while both isolated nanoparticles and agglomerates of platinum nanoparticles are found on the SKT surface. The CO conversion on the platinum catalysts supported on CNT reaches 100% at 400-450 °C, while the Pt/SKT catalysts are inactive and sinter during the reaction as seen in the TEM images for samples after use in catalysis. This result may be attributed to stabilization of the platinum nanoparticles on the CNT surface, which prevents their agglomeration during the reaction.

This work was carried out in a joint targeted basic research program of the National Academy of Sciences of Ukraine "Fundamental problems in the creation of new nanomaterials and nanotechnology."

REFERENCES

1. N. A. Baronskaya, T. P. Minyukova, A. A. Khasin, et al., *Usp. Khim.*, **79**, No. 11, 1112-1133 (2010).
2. E. Ya. Mel'nikov (ed.), *Nitrogen Technology Handbook* [in Russian], Vol. 1, Khimiya, Moscow (1986).
3. S. Lim, J. Bae, and K. Kim, *Int. J. Hydrogen Energy*, **34**, 870-875 (2009).
4. M. G. Castaño, T. R. Reina, S. Ivanova, et al., *J. Catal.*, **314**, 1-9 (2014).
5. B. Zugic, S. Zhang, D. C. Bell, et al., *J. Am. Chem. Soc.*, **136**, 3238-3245 (2014).

6. G. G. Olympiou, C. M. Kalamaras, C. D. Zeinalipour-Yazdi, and A. M. Efstathiou, *Catal. Today*, **127**, Nos. 1-4, 304-318 (2007).
7. M. Menon, A. N. Andriotis, and G. E. Froudakis, *Chem. Phys. Lett.*, **320**, 425-434 (2000).
8. K. C. Petallidou, K. Polychronopoulou, J. L. G. Fierro, and A. M. Efstathiou, *Appl. Catal. A*, in press (2015).
9. A. I. Tripol'skii, N. V. Lemesh, V. A. Khavrus', and P. E. Strizhak, *Teor. Éksp. Khim.*, **44**, No. 4, 228-232 (2008). [*Theor. Exp. Chem.*, **44**, No. 4, 240-244 (2008) (English translation).]
10. R. M. Rioux, H. Song, J. D. Hoefelmeyer, et al., *J. Phys. Chem.*, **109**, No. 6, 2192-2202 (2005).
11. Z. V. Kaidanovych, Ye. Yu. Kalishyn, and P. E. Strizhak, *Teor. Éksp. Khim.*, **48**, No. 6, 354-358 (2012). [*Theor. Exp. Chem.*, **48**, No. 6, 376-380 (2013) (English translation).]
12. S. C. Tsang, Y. K. Chen, J. F. Harrison, and L. H. Green, *Nature*, **372**, 159 (1994).
13. R. Buitrago, J. Ruiz-Martínez, J. Silvestre-Albero, et al., *Catal. Today*, **180**, 19-24 (2012).
14. T. K. Lee, J. H. Jung, J. B. Kim, and S. H. Hur, *Int. J. Hydrogen Energy*, **37**, 17992-18000 (2012).
15. A. A. Slinkin, *Usp. Khim.*, **60**, No. 4, 689-713 (1991).
16. Z.-T. Liu, Ch.-X. Wang, Z.-W. Liu, and J. Lu, *Appl. Catal. A*, **344**, 114-123 (2008).
17. A. Solhy, B. F. Machado, J. Beausoleil, et al., *Carbon*, **46**, 1194-1207 (2008).
18. Y. Zhao, Ch.-H. Li, and Zh.-X. Yu, *Mater. Chem. Phys.*, **103**, 225-229 (2007).
19. T. Onoe, S. Iwamoto, and M. Inoue, *Catal. Commun.*, **8**, No. 4, 701-706 (2007).